THE EFFECT OF MARTENSITE ON THE STRESS CORROSION CRACKING OF AUSTENITIC STAINLESS STEEL

K. Takashima*, N. W. Ringshall**, Y. Higo*, T. Obinata*,
T. Nakamura** and S. Nunomura*

*Reseach Laboratory of Precision Machinery and Electronics,
Tokyo Institute of Technology,
4259 Nagatsuta, Midori-ku, Yokohama, 227 Japan
**Technological University of Nagaoka, Nagaoka, 949-54 Japan

ABSTRACT

The effect of stress-induced martensite on the stress corrosion cracking of 304 stainless steel has been studied in 42% $MgCl_2$ solution at 130°C and 143°C. SCC crack growth in round-notched specimens containing martensite was much greater than in fully austenitic specimens under the same conditions, while this effect was not observed in fatigue precracked specimens. Fractographic observations showed that in round-notched specimens SCC cracks initiated along martensite bands, but then broke away to grow normal to the direction of maximum tensile stress. Cracks were then observed to grow across, rather than along, martensite bands, giving a characteristic lined fracture surface. Acoustic emission measurements indicated an active path corrosion mechanism for SCC crack growth in both austenitic and martensite-containing materials.

KEYWORDS

SCC; 304 stainless steel; austenite; martensite; round-notched; fatigue precracked; acoustic emission; active path corrosion.

INTRODUCTION

In recent years much research has been done on the stress corrosion cracking (SCC) of austenitic stainless steel with reference to the problems encountered during the operation of chemical and nuclear plant. During the cold-working or machining of austenitic stainless steel components, stress- and/or strain-induced martensite is introduced in the surface layer. This martensite phase is thought to affect subsequent stress corrosion of the material, but as yet there is some disagreement on the precise effect.

In the past it has been suggested (Edeleanu, 1953) that stress corrosion cracking in austenitic stainless steels followed the path of stress- and/or strain-induced martensite. However, this has met with some opposition. Hines and Hoar (1956) concluded that for the stress corrosion of 18-8 stainless steel smooth tensile specimens in boiling $MgCl_2$ solution, the presence of martensite influenced the crack initiation only. Re-analysis of later work by Hines (1961) indicates that for low volume fractions of martensite SCC occurs faster at low applied stresses, with

little effect of the martensite at high stresses, supporting an initiation effect. Recently Tamura and co-workers (1980) have analysed the effect of both α and ε martensite on the SCC of 304 stainless steel wire tensile specimens. However, the effects of martensite on initiation of SCC cracks and the subsequent propagation of the cracks have not as yet been considered separately.

In the present work the effects of initiation and propagation are studied by the use of fracture toughness specimens containing either a round notch or a sharp fatigue precrack, and the geometry of the SCC cracks is related to the morphology of stress-induced martensite at the notch or crack tip. In addition, acoustic emission monitoring was used to investigate whether the presence of stress-induced martensite affected the crack propagation mechanism.

EXPERIMENTAL METHOD

The material used was 10mm thick commercial grade 304 austenitic stainless steel plate. Two types of SCC specimens (DCB and constant-K) were machined from the plate, with their notch plane normals parallel to the rolling direction. The specimens were annealed for 1 hr at 1100°C in argon and furnace-cooled, giving a grain size of about 110μm. Following this, one of two kinds of pre-crack was introduced: a spark machined round notch of 0.125mm root radius; or a 3 mm length fatigue crack, grown at low loads. Both the spark-machined and fatigue crack lengths were controlled to ±20μm, the latter by the use of the potential drop technique, to ensure identical SCC crack growth conditions. Following precracking the specimens were heat-treated for 1 minute at 600°C, as registered on a probe inside the specimen, to remove stress-induced martensite introduced during the precracking.

The precracked specimens were divided into two batches: A, which were fully austenitic; and M, which contained stress-induced martensite at the crack tip. This stress induced martensite was produced by preloading austenitic specimens at -78°C to a crack tip stress intensity of 30MPa$\sqrt{m}$. This gave a localised transformed region in the crack tip plastic zone, along the direction of maximum resolved shear stress.

Stress corrosion tests were carried out at constant load in 42% $MgCl_2$ solution at 130°C and 143°C (Boiling), using a horizontal cantilever-type creep machine. Temperature control was ±1°C. The crack length was monitored using the change in specimen compliance with crack length, measured by a clip-gauge. In addition, acoustic emission (AE) was monitored during the 130°C tests, where external noise levels from the solution, etc., were low. Following testing, the specimens were fractured by fatigue, and the crack morphology and corrosion fracture surface observed optically and in the SEM.

The acoustic emission monitoring system consisted of three channels, using resonant PZT transducers with resonant frequencies of 15kHz, 140kHz and 1MHz respectively, connected to the specimen by waveguides. RMS level and ringdown and event counts were monitored in each channel, and the event amplitude distributions were measured using a peak voltmeter and peak height analyser. The use of three frequency ranges allowed the discrimination of external noise sources, which because of test geometry could not be removed by spatial filtering or guard transducers. Careful test design gave less than 10 noise events/hour above a 10μV threshold.

RESULTS AND DISCUSSION

Figure 1 shows sections through the middle of round-notched specimens, both fully austenitic (A) and with a crack tip martensite-transformed region (M), after 4 hr in boiling 42% $MgCl_2$ solution at 6kN load. It can be seen that the crack length in

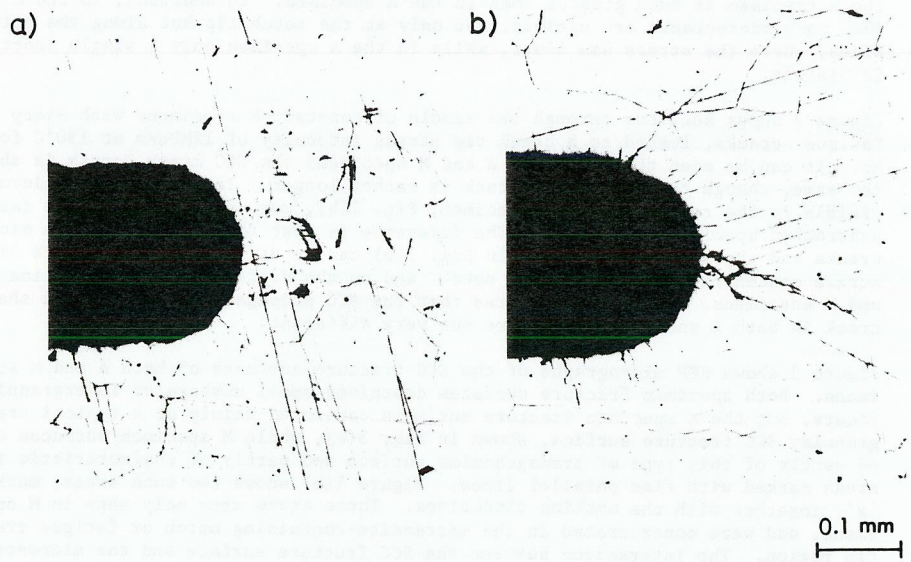

Fig. 1. Stress corrosion cracks initiated from rounded notches.
a) Austenitic (A) specimen
b) Martensite-containing (M) specimen

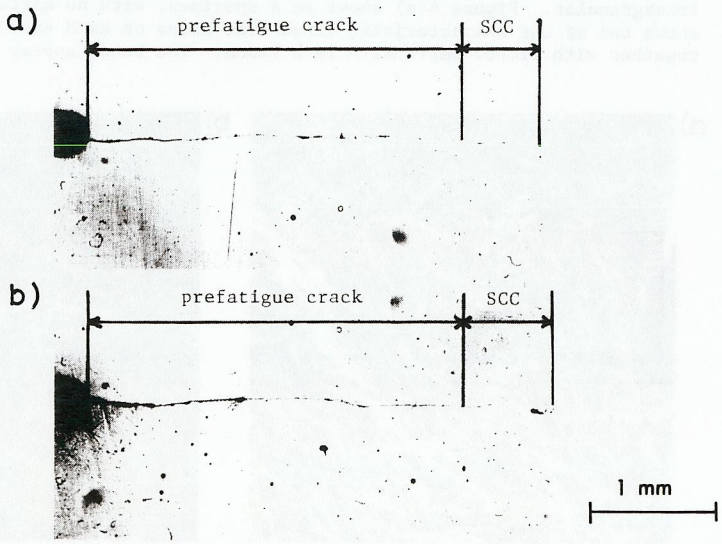

Fig. 2. Stress corrosion cracks initiated from fatigue precracks.
a) Austenitic (A) specimen
b) Martensite-containing (M) specimen

the M specimen is much greater than in the A specimen. In addition, in the M specimen many microcracks are visible, not only at the notch tip but along the notch sides, where the stress was lower, while in the A specimen only a single short crack is visible.

Figure 2 shows sections through the middle of constant-K specimens with sharp prefatigue cracks, loaded to a crack tip stress intensity of 12MPa$\sqrt{m}$ at 130°C for 33 hr. It can be seen that for both A and M specimens the SCC crack length is about the same, though the M specimen crack is rather longer. In addition the microcracks visible in the round-notched M specimen, Fig. 1(b), are not visible in the fatigue-precracked specimen, Fig. 2(b). The inference is that the presence of the microcracks and the shorter SCC crack in Fig. 1(b) can be attributed to the more diffuse stress concentration of the round notch, and to the different initiation time in A and M specimens. Figure 2 indicates that the SCC propagation rates from a sharp crack in both A and M specimens are not very different.

Figure 3 shows SEM micrographs of the SCC fracture surfaces of both A and M specimens. Both specimen fracture surfaces contained small numbers of intergranular facets, but the A specimen fracture surfaces consisted mainly of a typical transgranular SCC fracture surface, shown in Fig. 3(a), while M specimen surfaces consisted partly of this type of transgranular surface and partly of characteristic flat areas marked with fine parallel lines. Figure 3(b) shows two such areas, marked 'x', together with the marking directions. These areas were only seen in M specimens, and were concentrated in the martensite-containing notch or fatigue crack tip region. The interaction between the SCC fracture surface and the microstructure was investigated by protecting the fracture surface with metal-filled acrylic, sectioning the specimen normal to the fracture surface at mid-thickness, and polishing, and etching to show the microstructure and martensite. On stripping the protective acrylic, the interface between the etched microstructure and the fracture surface could be observed in the SEM, Fig. 4. In both A and M specimens the SCC cracks were transgranular. Figure 4(a) shows an A specimen, with no martensite, and Figure 4(b) shows one of the characteristic lined flat areas on an M specimen ('x' in Fig. 3(b)), together with etched martensite lath bands. The bands appear curved here due to

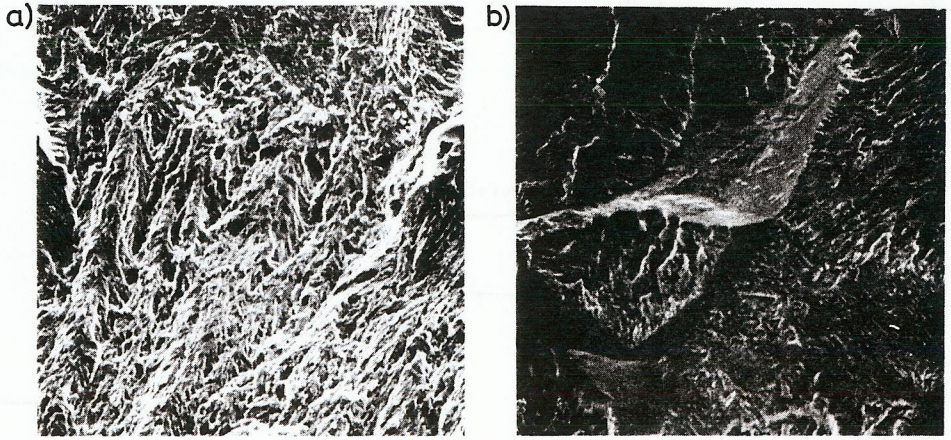

Fig. 3. SEM micrographs of SCC fracture surfaces.
a) Austenitic (A) specimen
b) Martensite-containing (M) specimen

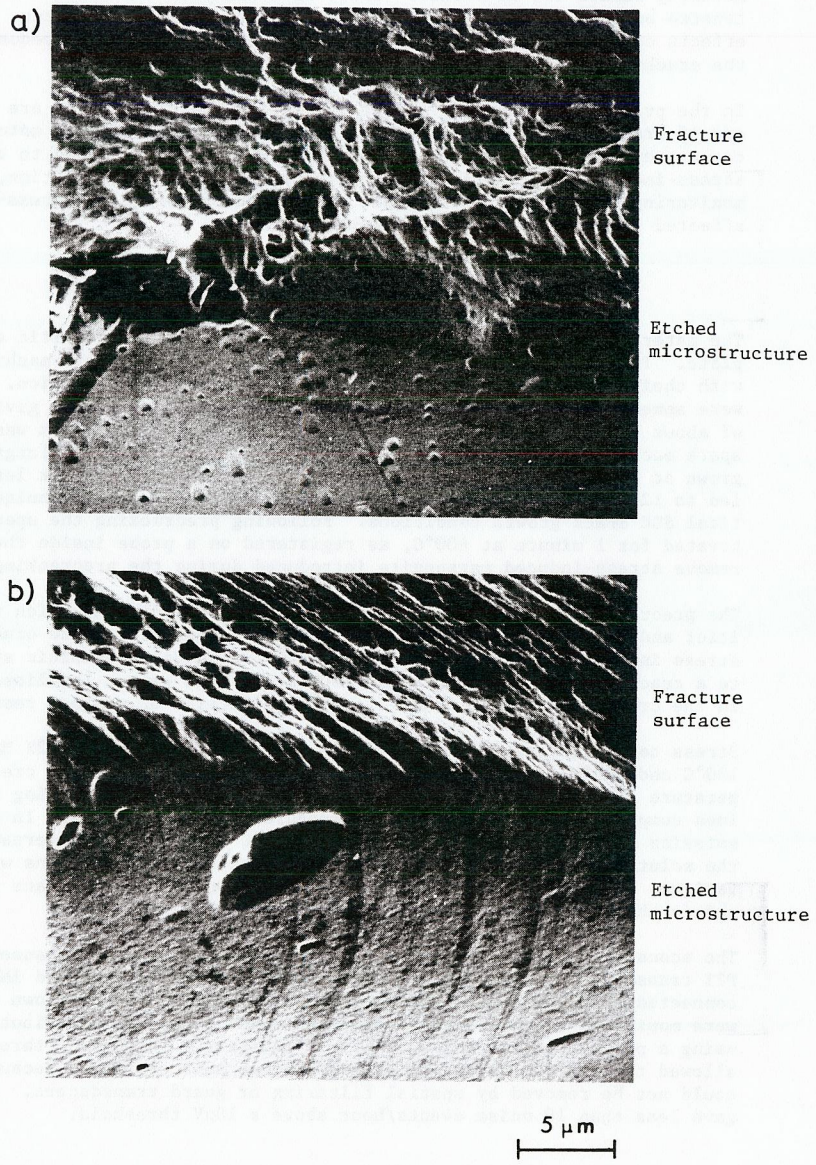

Fig. 4. SEM micrographs showing the interface between the mid-thickness SCC fracture surface and the microstructure, etched to show martensite.
a) Austenitic (A) specimen
b) Martensite-containing (M) specimen

rounding of the edge during polishing. It can been seen that the lines are due to the SCC crack growing across the martensite bands, and that the crack does not appear to grow along martensite bands.

The acoustic emission recorded during SCC crack propagation was found not to vary with frequency, or between A and M specimens, and was close to the background noise level. This is consistent with an active path corrosion mechanism in both austenite and martensite (Okada, 1976). Figure 5 shows 140kHz cumulative event rate amplitude distributions for A and M specimens, measured over a 3 hr period. The event rate for amplitudes greater than 10μV is less than 10/hr, which rules out hydrogen-induced microcracking in the BCC martensite phase, rapid tearing of the ligaments between selectively dissolved martensite bands, or further stress-induced martensite transformation at the crack tip as significant mechanisms.

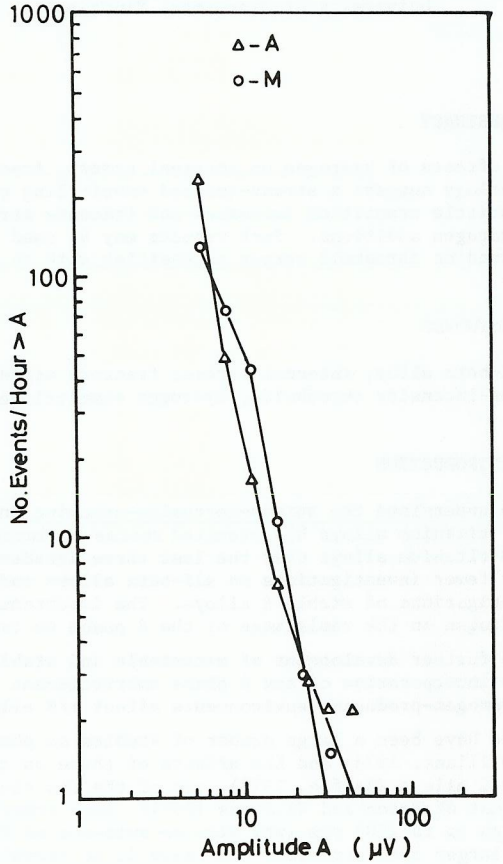

Fig. 5. Cumulative event rate amplitude distributions for 140kHz acoustic emission during SCC crack propagation.
A: Austenitic specimen
B: Martensite-containing specimen

The effect of martensite on SCC initiation was investigated by examining the notch root of round notched specimens, etched to show martensite. Figure 6 shows an SEM micrograph of the mid-thickness section of an M specimen notch root and etched microstructure, containing martensite lath band orientation M_1 and M_2, microcrack C_1, and the main SCC crack C_2. The microcrack C_1 appears to be parallel to martensite band orientation M_1, and the initial section of C_2 parallel to M_2. However, after growing about 20μm, C_2 breaks away from the M_2 direction to grow normal to the direction of maximum stress. This effect was also observed in the optical microscope for both microcracks and main cracks in M round notched specimens, but not in the fatigue cracked M specimens. The inference is thus that initiation occurs by selective corrosion of martensite bands, but that after initiation the crack follows the direction of maximum stress, regardless of martensite orientation. In the present work the martensite volume fraction was small, and the above would not necessarily be true for large volume fractions, where the probability of finding a martensite band close to the normal to the maximum stress direction is high.

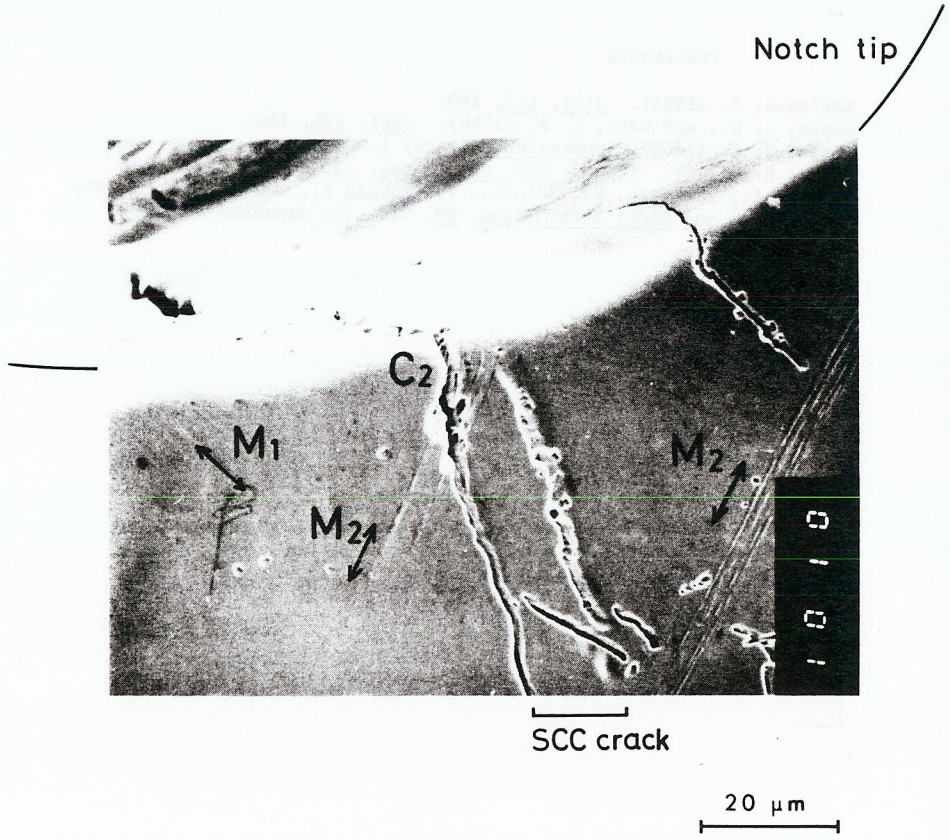

Fig. 6. SEM micrograph showing the initiation of SCC cracks in the mid-thickness of a round notched martensite-containing (M) specimens, etched to show martensite. Cracks are marked C, and martensite band orientations indicated by M.

CONCLUSION

The effect of stress-induced martensite on the stress corrosion cracking of 304 stainless steel in 42% $MgCl_2$ solution at 130°C and 143°C has been studied, and the following conclusions made:

1. The SCC crack length in round-notched specimens containing martensite was much longer than in fully austenitic specimens under the same conditions, while this difference was not observed in fatigue-precracked specimens.
2. Fractographic observations showed that in round-notched specimens SCC cracks initiated along martensite bands, but then broke away to grow normal to the direction of maximum tensile stress. Cracks were then observed to subsequently grow across, rather than along, martensite bands, giving a characteristic lined fracture surface.
3. Acoustic emission measurements indicated an active path corrosion mechanism for SCC crack growth in both austenitic and martensite-containing material.

REFERENCES

Edeleanu, C. (1953). JISI, 173, 140.
Hines, J. G., and Hoar, T. P. (1956). JISI, 184, 166.
Hines, J. G. (1961). Corrosion Science, 1, 2.
Okada, H. (1976). J. Mat. Sci. Soc. Japan, 13, 24. (in Japanese)
Tamura, I., Takizawa, K., Shimizu, Y., Yoneda E., and Shoji H. (1980). J. Iron and Steel Inst. Japan, 66, 514. (in Japanese).